[4]Akselvoll, K., and Moin, P., "Large-Eddy Simulation of Turbulent Confined Coannular Jets," *Journal of Fluid Mechanics*, Vol. 315, 1996, pp. 387–411.

[5]Sommerfeld, M., Ando, A., and Wennerberg, D., "Swirling, Particle-Laden Flows Through a Pipe Expansion," *Journal of Fluids Engineering*, Vol. 114, No. 4, 1992, pp. 648–656.

[6]Roback, R., and Johnson, B. V., "Mass and Momentum Turbulent Transport Experiments with Confined Swirling Coaxial Jets," NASA CR-168252, Aug. 1983.

K. Kailasanath
Associate Editor

Prediction of Shock Angles Caused by Sharp Delta Wings with Attack Angle

S. Koide*
Japan Defense Agency, Tokyo 154, Japan
and
A. F. Loria† and H. Babinsky‡
Cambridge University,
Cambridge CB2 1PZ, England, United Kingdom

Introduction

FOR glancing shock-wave/turbulent-boundary-layer interactions, the inviscid shock wave has an important role for specifying the interaction behavior regardless of the shape of the shock generator.[1] Hence, the trace of the shock wave on the wall provides an important reference position (the imaginary position that would exist if no boundary layer were presented on the wall) for understanding the interaction. The first author recently proposed empirical prediction methods for the shock angles caused by a series of rhombic delta wings (RDWs) at zero angle of attack[2] (Fig. 1a) and flat delta wings (FDWs) with angle of attack[3] (Fig. 1b). Using these methods, the shock angle on the plane of symmetry of the wing, β, can be predicted easily. This angle also specifies the trace of a shock wave along the wall when a swept sharp fin (the half-cut model of the RDW or FDW) is placed on the wall (equivalent to the position of the plane of symmetry for the wing). In this Note, the two methods are combined to predict the shock angles for sharp delta wings (SDWs) with angle of attack, in which both the RDWs and FDWs are included (Fig. 1c). Using the combined method, one can specify the trace of the shock generated by a swept sharp fin on the wall for various angles of attack α, sweep angles λ, half-apex angles ε, and Mach numbers M.

Summary of the Shock-Angle Prediction Methods for RDWs at Zero α and FDWs with α

For the RDWs at zero α, Ref. 2 suggested the following approach: The shock angles β_{RDW} obtained computationally and experimentally at various M, ε, and λ were nondimensionalized by the parameter $[\beta_{\mathrm{RDW}}/\beta_{\mathrm{OS}}(\varepsilon)] \cdot 2\zeta/(\pi M^a)$ and were plotted against $\zeta = \tan^{-1}[1/(\sin\varepsilon \tan\lambda)]$ (in radians; see Fig. 1a). In the parameter, the power a is $(\pi/2 - \zeta)/3$ and $\beta_{\mathrm{OS}}(\varepsilon)$ is the theoretical two-dimensional oblique shock angle for a flow deflection ε. To correlate the parameter against ζ, a fourth-order, least-squares equation was obtained:

$$F(\zeta) = -0.2504 + 0.8081\zeta - 0.1829\zeta^2 - 0.0971\zeta^3 + 0.1318\zeta^4 \tag{1}$$

Received Feb. 2, 1998; revision received March 10, 1998; accepted for publication March 25, 1998.

*Senior Research Engineer, Technical Department, Technical R&D Institute, 1-2-24 Ikejiri, Setagaya. Member AIAA.

†Mechanical Engineering Student, Department of Engineering, Trumpington Street.

‡Lecturer in Aerodynamics, Department of Engineering. Member AIAA.

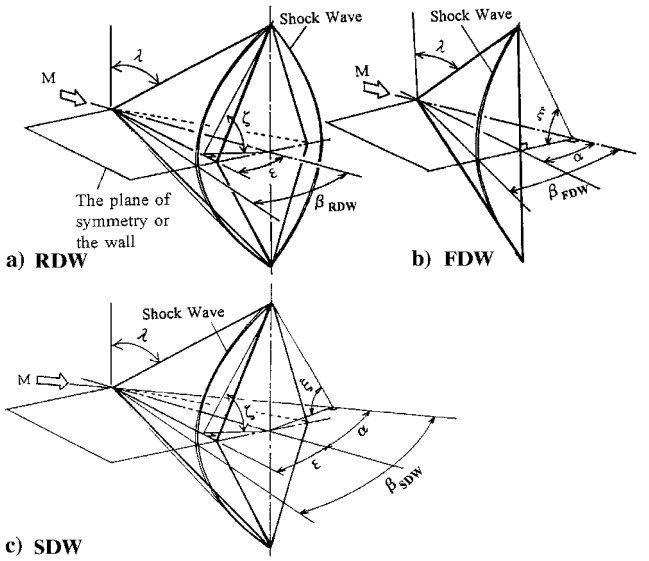

Fig. 1 Schematic views.

The value of β_{RDW} is then determined directly from

$$\beta_{\mathrm{RDW}} = \pi\beta_{\mathrm{OS}}(\varepsilon)F(\zeta)M^a \Big/ (2\zeta) \tag{2}$$

Similarly, the shock angle for the FDWs with α can be predicted by[3]

$$\beta_{\mathrm{FDW}} = \pi\beta_{\mathrm{OS}}(\alpha)G(\xi)M^b \Big/ (2\xi) \tag{3}$$

where ξ is $\tan^{-1}[1/(\sin\alpha \tan\lambda)]$ (in radians; see Fig. 1b), the power b is $(\pi/2 - \xi)/3$, and $G(\xi)$ has been chosen as

$$G(\xi) = -0.0202\xi + 1.0204\xi^2 - 0.8885\xi^3 + 0.3234\xi^4 \tag{4}$$

Prediction of the Shock Angles for SDWs with α

The shock angle for SDWs with angle of attack may be expressed by the combination of the two angles, i.e., $\beta_{\mathrm{SDW}} = f(\beta_{\mathrm{RDW}}, \beta_{\mathrm{FDW}})$. To construct a prediction method for β_{SDW}, one has to consider the following conditions. 1) When α approaches 0 deg, β_{SDW} has to approach β_{RDW}. 2) When ε approaches 0 deg, β_{SDW} has to approach β_{FDW}. 3) When λ approaches 0 deg, β_{SDW} has to approach $\beta_{\mathrm{OS}}(\alpha + \varepsilon)$ (see Fig. 1). To satisfy these conditions, the relationship

$$\beta_{\mathrm{SDW}} = \beta_{\mathrm{FDW}}\beta_{\mathrm{RDW}}\beta_{\mathrm{OS}}(\alpha + \varepsilon)/[\beta_{\mathrm{OS}}(\alpha)\beta_{\mathrm{OS}}(\varepsilon)] \tag{5}$$

has been introduced. It can be seen from Eqs. (2) and (3) that β_{RDW} and β_{FDW} become $\beta_{\mathrm{OS}}(\varepsilon)$ and $\beta_{\mathrm{OS}}(\alpha)$, respectively, when λ approaches 0 deg, and both of them become the Mach angle $[\mu = \sin^{-1}(1/M)]$ when ε and α approach 0 deg. Hence Eq. (5) satisfies conditions 1–3.

To check the validity of Eq. (5), parametric experiments have been carried out at Cambridge University's 21×11 cm^2 supersonic wind tunnel. Eight RDWs varying in sweep ($\lambda = 45$–73 deg) and half-apex angle ($\varepsilon = 6$–14 deg) were tested over three Mach numbers (1.8, 2.5, and 3.5 with an error of $\pm 1\%$), while the angle of attack was varied in 5-deg steps ($\alpha = 5$–20 deg). The shock angles were measured from shadowgraph images. The optical setup was adjusted to maximize the measurement accuracy. Nevertheless, an error of 2% of the angle was determined as an upper limit.

Figure 2 shows experimentally obtained values of β_{SDW} against angles predicted by Eq. (5). It can be seen that the agreement between experiment and prediction is very good; 80% of the predictions lie within 2 deg of the experimental values, and 50% are within 1 deg. However, some of the predicted values can be seen to depart from the solid line. Most of these are where $\lambda \geq 70$ deg at the lower Mach numbers of 1.8 and 2.5 (see the triangle points in Fig. 2). Under such conditions, the shock wave is nearly circular, and therefore the prediction using β_{OS} deteriorates. However, even for λ above 70 deg,

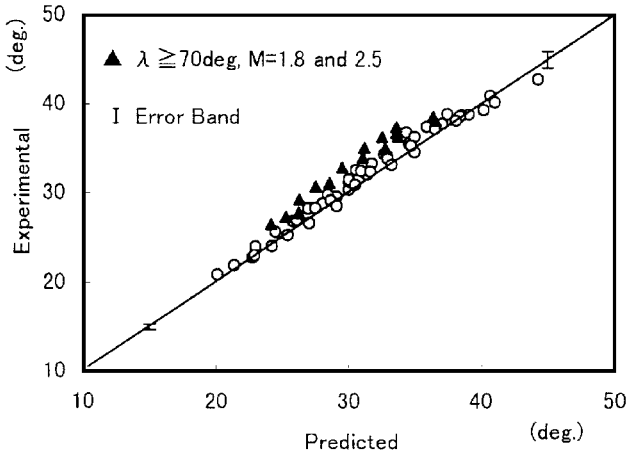

Fig. 2 Comparison of the predicted and experimentally obtained shock angles.

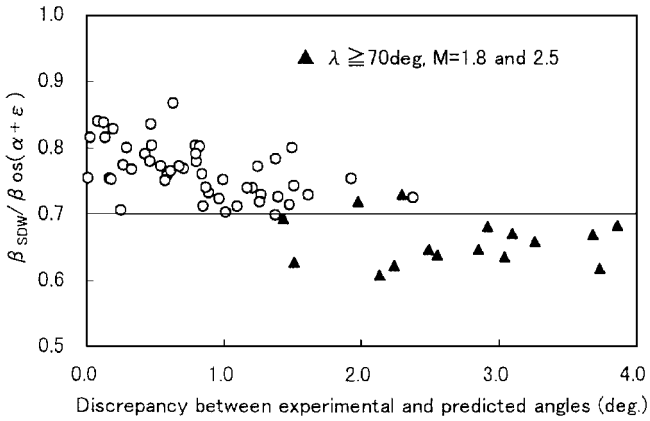

Fig. 3 Shock-curvature effect on discrepancy between experimental and predicted angles.

the prediction improves when the shock becomes flatter at the higher Mach number of 3.5. This shock-curvature effect can be evaluated by a simple nondimensional shock angle, $\beta_{SDW}/\beta_{OS}(\alpha+\varepsilon)$, which indicates a deviation of the SDW shock wave from the planar two-dimensional shock. Figure 3 plots discrepancies between experimental and predicted angles against the nondimensional shock angles. Most of the triangle points fall where $\beta_{SDW}/\beta_{OS}(\alpha+\varepsilon)$ is less than 0.7. If all of the cases less than 0.7 are excluded, then most of the predictions fall within the experimental accuracy shown by the bars in Fig. 2.

Conclusion

It can be concluded that the proposed method is practically accurate enough as long as $\beta_{SDW}/\beta_{OS}(\alpha+\varepsilon)$ is above 0.7. Finally, this procedure can be applied regardless of whether the shock is attached at the leading edge (Fig. 1 shows the attached case only); however, the procedure is not applicable for the cases in which any of α, ε, and $\alpha+\varepsilon$ is above the theoretical attachment limit for the two-dimensional oblique shock at a certain M because β_{OS} is not obtainable for Eq. (5) under such a condition.

References

[1]Koide, S., Saida, N., and Ogata, R., "Correlation of Separation Angles Induced by Glancing Interactions," *AIAA Journal*, Vol. 34, No. 10, 1996, pp. 2198–2200.

[2]Koide, S., Griesel, C. J. W., and Stollery, J. L., "Correlation of Shock Angles Caused by Rhombic Delta Wings," *AIAA Journal*, Vol. 34, No. 7, 1996, pp. 1529–1531.

[3]Koide, S., "Correlation of Shock Angles Caused by Flat Delta Wings," *AIAA Journal*, Vol. 34, No. 9, 1996, pp. 1956–1958.

M. Samimy
Associate Editor

Observations of Supersonic Flat Plate Wake Transition

N. T. Clemens* and M. F. Smith†
University of Texas at Austin, Austin, Texas 78712-1085

I. Introduction

ALTHOUGH the instability and transition of supersonic slender body wakes have seen extensive study for decades, little is known of the topology of the developing vortical structures. Kendall studied the stability of Mach 2–4 flat plate wakes and found that in a quiet wind tunnel, where all wall boundary layers remained laminar, the wake underwent aperiodic transition, i.e., without an identifiable vortex street. In contrast, in a noisy tunnel, where the wall boundary layers were turbulent, a periodic vortex street was observed. In a more recent study, Chen et al.[1] studied three-dimensional time-developing supersonic planar wakes using direct numerical simulation and observed the development of large-scale, three-dimensional structures that are similar to those previously observed in incompressible flat plate wakes.[2]

In this Note, we discuss the results of a primarily flow visualization investigation of the development of instabilities in the near-field region of a Mach 3 flat plate wake. Additional experimental details and results can be found in Ref. 3.

II. Experimental Apparatus and Run Conditions

The experiments were conducted in a pressure-vacuum wind tunnel with a freestream Mach number of 3.0. The test section had a 51×51 mm cross section and a length of 310 mm. The wake was formed using a splitter plate (3-deg full angle and 0.7-mm tip thickness) that began upstream of the nozzle throat and extended 50 mm into the test section. The primary diagnostic method used was planar laser scattering (PLS) from a seeded alcohol fog. The fog was illuminated with a light sheet from a frequency-doubled Nd:YAG laser, and the images were acquired using a charge-coupled device video camera.

Results are presented for stagnation and test section static pressures of 80 ± 4 kPa and 2 ± 0.02 kPa absolute, respectively, a stagnation temperature of 290 ± 3 K, a freestream Mach number of 3.0, and a Reynolds number based on plate length from the throat of $Re_L = 1.4 \times 10^6$. The splitter plate boundary layers were laminar and were measured with a pitot tube (with a sharp flattened tip, 0.3 mm high × 1 mm wide) to have a thickness of $\delta_{99} = 1.9 \pm 0.1$ mm. The side wall boundary layers were transitional, probably owing to being tripped by test section/nozzle and test section/window junctions.

III. Results

Mean pitot pressure profiles across the wake were obtained at several downstream locations. The pitot pressure measurements were converted to velocity profiles using the Rayleigh pitot formula and the assumption of adiabatic flow. The wake momentum thickness was computed from these profiles to be $\theta = 0.3 \pm 0.02$ mm at all stations. As a means of quantifying the level of compressibility in the wake, the relative Mach number defined as $M_r = (U_\infty - U_c)/a_\infty$ is used, where U_∞ is the freestream velocity, U_c is the wake centerline velocity, and a_∞ is the freestream sound speed. The relative Mach number variation as a function of downstream position is shown in Fig. 1. The coordinate system is defined to have the x, y, and z coordinates as representing the streamwise, cross-stream, and

Presented as Paper 96-0785 at the AIAA 34th Aerospace Sciences Meeting, Reno, NV, Jan. 15–18, 1996; received Sept. 20, 1997; revision received March 17, 1998; accepted for publication March 18, 1998.

*Assistant Professor, Department of Aerospace Engineering and Engineering Mechanics. Senior Member AIAA.

†Graduate Student, Department of Aerospace Engineering and Engineering Mechanics.